Journal of The Electrochemical Society, **152** (1) G50-G56 (2005)
0013-4651/2004/152(1)/G50/7/$7.00 © The Electrochemical Society, Inc.

Process Improvement and Reliability Characteristics of Spin-On Poly-3-hexylthiophene Thin-Film Transistor

Shuo-Cheng Wang,[z] Jen-Chung Lou, Bo-Lin Liou, Ron-Xion Lin, and Ching-Fa Yeh

Department of Electronics Engineering and Institute of Electronics, National Chiao-Tung University, Hsinchu, Taiwan

Poly-3-hexylthiophene (P3HT) based thin-film transistors were fabricated. Various spin-coating conditions including spin speeds, curing temperatures, solvents, and weight percentages of P3HT have been examined. It was found that the P3HT of 0.3 wt % dissolved in chloroform contributes to the lowest surface roughness and the highest ON/OFF current ratio over four orders of magnitude. Besides, the anomalous gate leakage current was eliminated successfully by growing a thick field oxide layer in the source/drain regions. Through O_2, N_2, H_2O, or high-vacuum treatments, it was confirmed that the threshold voltage and mobility of organic devices degrades rapidly when the P3HT-based organic thin-film transistors were exposed to the O_2 atmosphere within 8 h. Moreover, the threshold voltage increases under a positive gate bias stress while the V_{th} decreases after a negative gate bias stress. The mechanism was attributed to the polarization effect of P3HT film.
© 2004 The Electrochemical Society. [DOI: 10.1149/1.1829417] All rights reserved.

Manuscript submitted November 21, 2003; revised manuscript received June 28, 2004. Available electronically November 22, 2004.

The field of organic electronics has received considerable attention, because of the wide range of applications in identification tags, light-emitting devices, transistors, photovoltaic cells, photodetectors, and flat panel displays.[1-6] Soluble organic semiconductors have attracted particular interest, since these materials can be easily spun-coated to form circuits for disposable electronics on a plastic substrate, with the advantages of a large-area coverage, structural flexibility, low-temperature fabrication processing, and especially low cost.[7,8] Of various soluble organic semiconductors currently in use, poly-3-hexylthiophene, P3HT, has become the most promising candidate for all-organic semiconductor integration due to its easy synthesis and relatively high mobility ($\sim 10^{-2}$ cm^2/Vs).[9]

However, several issues should be addressed before P3HT-based organic thin-film transistors (OTFTs) can be employed. For example, since P3HT is generally solution-processed, the conditions of spin-coating including the solvents, the weight percentages of P3HT, and the curing temperatures, etc., should be optimized to acquire satisfactory electrical properties of OTFTs. Besides, the anomalous leakage current through the gate dielectric may reduce the ON/OFF current ratio and increase power consumption.[8] Furthermore, the organic materials are well known to be environmentally and electrically unstable. It is well-documented that oxygen would form a weakly bound donor-acceptor complex (charge-transfer complex) with P3HT or localized states within the $\pi - \pi^*$ gap.[10,11] For oligomers such as pentacene, H_2O molecules can easily diffuse into the crevices of pentacene film, interacting with the trapped carriers at the grain boundaries, causing the degradation of hole mobility or the threshold voltage shift.[12,13] Additionally, a significant threshold voltage shift under the gate bias stress was also reported.[14-16] Nevertheless, the impact of the atmosphere or stress on the electrical characteristics of P3HT based OTFTs has not been extensively examined.

In this investigation, P3HT was used as an active layer of OTFTs. The origin of anomalous leakage current was clarified while an isolation structure was verified to be effective for eliminating the leakage path. The finished OTFTs were treated under different ambient conditions or various applied stress voltages to examine the reliability characteristics in an electrical point of view. Fundamental physical tests, including the surface roughness or film thickness were also conducted under different spinning or curing conditions.

Experimental

The P3HT organic TFTs were fabricated on a heavily doped n^+ silicon substrate with thermally grown gate insulator and thick field oxide, as shown in Fig. 1a. First, phosphorus atoms were diffused into an n-type Si wafer by $POCl_3$ to create a common gate electrode. A field SiO_2 layer with a thickness of 500 nm and a thin gate oxide layer with a thickness of 100 nm were subsequently grown in a furnace. Afterward, source/drain regions were defined using a photolithography process followed by the thermal evaporation of a 20 nm thick layer of Ti as an adhesion layer and a 100 nm thick layer of Pt as a contact material. The wafer was then immersed in acetone to lift off the photoresist and form the source/drain regions. A comb geometry, as depicted in Fig. 1b for the source/drain (S/D) contacts, was adopted to minimize the device area and the associated gate to source/drain leakage current. Further, an OTFT structure without a field oxide layer was also fabricated for comparison (Fig. 1c). A typical channel width W was in the range of 100-10,000 μm and a channel length was 10-50 μm.

The samples, after S/D patterning, were treated with hexamethyldisilazane (HMDS) to improve adhesion and regioregularity between the polymer chain and the oxide surface.[17] Next, P3HT of 0.1, 0.3, 0.8 or 2.0 wt % dissolved in chloroform or xylene was filtered through a 0.2 μm pore-size PTFE filter and then spun onto the wafer surface, which was then cured at 120°C. Here the atomic force microscope (AFM) was also utilized to observe the surface morphology of P3HT deposited with different weight percentages, spin speeds and curing temperatures. P3HT and its solvent were both purchased from Aldrich chemical company, and no further purification or sublimation was performed.

To examine the reliability characteristics of the finished OTFTs, the samples were first stored in a vacuum chamber under base pressure of 10^{-6} Torr for two days and then treated with O_2 gas or N_2 gas in a furnace (flow rate, 5 l/min) or immersed in DI water for 0-19 h at room temperature. After various treatment processes, the electrical characteristics of OTFTs were measured immediately in the atmosphere using an HP4156 semiconductor parameter analyzer. Besides, a gate bias of ±25 V was applied to evaluate the electrical characteristics of OTFTs under stress.

Results and Discussion

Optimization of spin-on conditions of P3HT.—Figure 2a exhibits the surface morphology of the deposited P3HT film for P3HT of 0.3 wt % in xylene. Many clusters of undissolved P3HT powder, despite having been filtered, are still observed. For P3HT dissolved in chloroform, however, no microparticles of P3HT can be found as shown in the AFM photographs of Fig. 2b-e even at the P3HT wt % as high as 2.0. Besides, the rms value of surface roughness reaches 0.82 nm at 0.3 wt % and then increases significantly at 0.8 and 2.0 wt %. Pin holes are commonly observed in Fig. 2e, which may attribute to the sudden evaporation of solvents through a thick P3HT layer. No ap-

[z] E-mail: scwang.ee88g@nctu.edu.tw

Downloaded on 2014-04-26 to IP 140.113.38.11 address. Redistribution subject to ECS terms of use (see ecsdl.org/site/terms_use) unless CC License in place (see abstract).

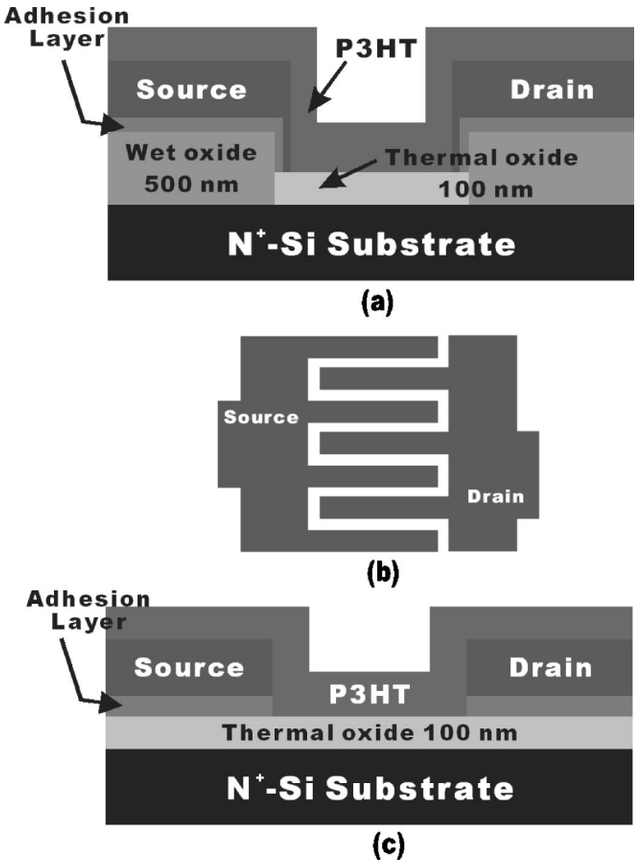

Figure 1. Schematic diagram of OTFT with (a) the field oxide layer on the source/drain region, (b) comb structures for source/drain electrodes, and (c) a conventional structure.

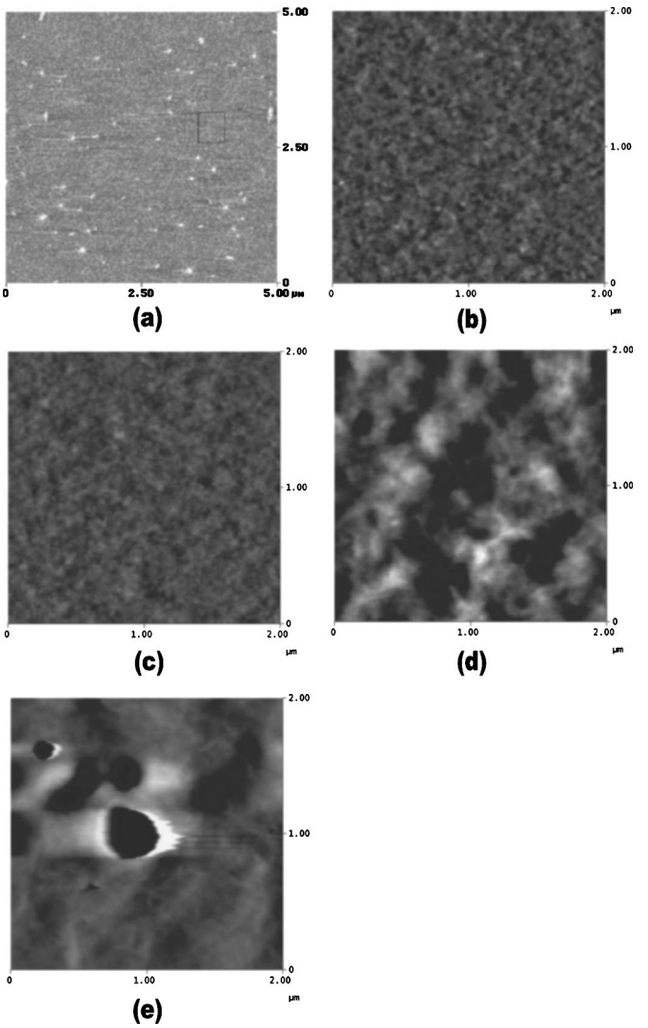

Figure 2. Surface morphology measured by AFM of the P3HT films deposited with different conditions: (a) 0.3 wt % in xylene, (b) 0.1 wt % in chloroform, (c) 0.3 wt % in chloroform, (d) 0.8 wt % in chloroform, and (e) 2.0 wt % in chloroform.

parent grain/grain-boundary structure was found in the AFM photographs because the P3HT thin film is a long-chain polymer with a lamella layer structure.[17]

Table I summarizes the surface roughness of the P3HT film (dissolved in xylene) with respect to spin speed and the postannealing temperature. The surface roughness of the P3HT film slightly declines as the spin speed increases, since a higher spin speed results in a better distribution of the solvent and, therefore, a smoother surface. For surface roughness of P3HT after postannealing, although the melting temperature of P3HT is 178°C, increasing the film to a moderately similar temperature is expected to thermodynamically allow a change triggered by a conformation change within the alkyl group. Mattis *et al.* found that the roughness was increased after a high-temperature annealing step, indicating that the P3HT film was rearranged into a more disorganized state.[10] Nevertheless, the postannealing temperature (up to 170°C) negligibly affects the surface roughness, according to the experimental results presented herein. The authors speculated that the deposited P3HT film with xylene as a solvent is too thin to reflect the conformation change of P3HT polymers in the surface morphology.

At a spin speed of 2000 rpm, the thickness of P3HT film deposited by xylene solution (0.3 wt %) was 240 Å, which is much thinner than that deposited by chloroform (0.3 wt %, 1140 Å). Both of them were estimated from the cross-sectional view (not shown) obtained using the scanning electron microscope (SEM). Other optical methods such as ellipsometry or spectrometry, however, were not appropriate for measuring the thickness due to the nonregioregularity and the associated nonuniformity of the refractive index of P3HT.

Figure 3 compares the I_S-V_G and the mobility curves of OTFTs fabricated by different solvents. The field-effect mobility of OTFTs deposited by chloroform and xylene are 2.1×10^{-3} and 7.0×10^{-4} $cm^2/V\,s$, respectively. Based on the above observation that the thickness of P3HT prepared by xylene solution is only 240 Å, the resulting inferior mobility is due to the poor step coverage of

Table I. Surface roughness of the P3HT film with respect to spin speed and the postannealing temperature.

Spin speed (rpm)	Surface roughness of P3HT film (nm)
1000	0.45
2000	0.40
4000	0.39
6000	0.36
Annealing temperature	Surface roughness of P3HT film (nm)
Room temperature	0.53
100°C	0.32
150°C	0.41
170°C	0.36

Downloaded on 2014-04-26 to IP 140.113.38.11 address. Redistribution subject to ECS terms of use (see ecsdl.org/site/terms_use) unless CC License in place (see abstract).

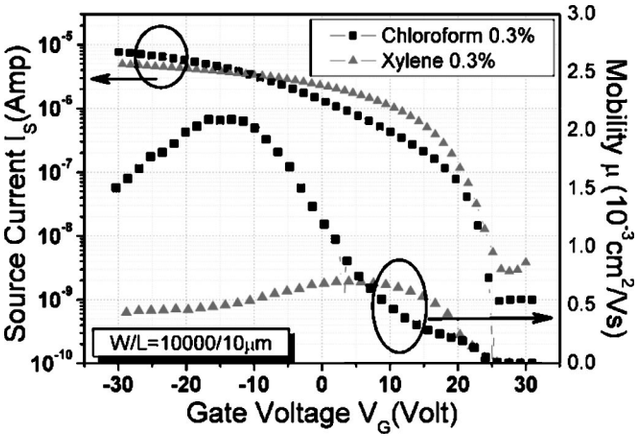

Figure 3. I_S-V_G and mobility curves of the OTFTs fabricated by xylene or chloroform solution.

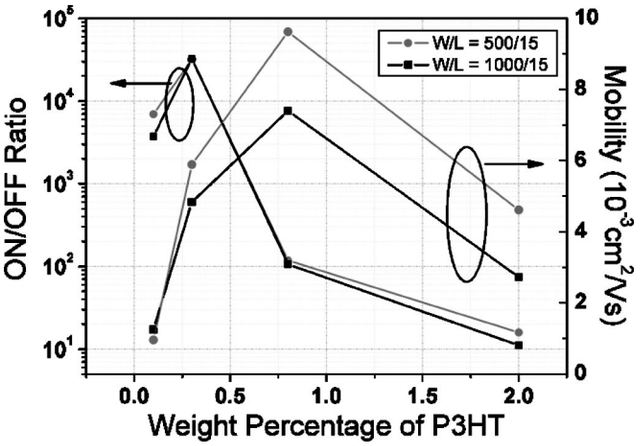

Figure 5. ON/OFF current ratio and mobility characteristics of OTFTs *vs.* various weight percentages of P3HT film.

P3HT film on the S/D electrodes, disordered lamella structure, and strong surface scattering effect owing to the vertical gate electric field. Nevertheless, the gate controllability is enhanced for a thin active layer and thus the subthreshold swing of devices prepared by xylene solution becomes steeper than those prepared by chloroform. Since chloroform is toxic to the neural system and its usage is restricted or prohibited in some countries, xylene becomes an appropriate choice despite its low mobility and solubility to P3HT.[18]

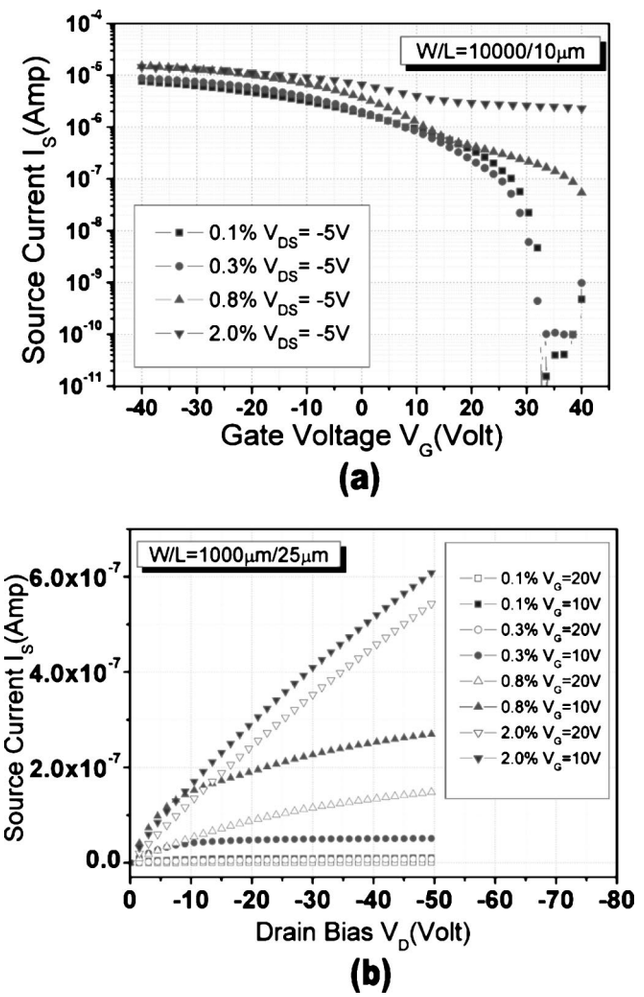

Figure 4. (a) I_S-V_G and (b) I_S-V_D curves of the OTFTs fabricated by different weight percentages of P3HT in chloroform.

Figure 4a illustrates the I_S-V_G curves of OTFTs fabricated by different weight percentages of P3HT in chloroform. The OTFTs exhibit satisfactory ON/OFF ratio, subthreshold swing and leakage current for the concentration of P3HT below 0.3%. However, the ON/OFF current ratio of 0.8 and 2.0% samples reduced drastically to less than 10, primarily resulting from the increase of the leakage current. Figure 4b shows the I_S-V_D characteristics of OTFTs in their OFF state when a positive gate bias was applied. As the gate voltage increases, the channel would deplete while the off-current, I_S, gradually saturates, and thus I_S becomes independent of the drain voltage. Nevertheless, the I_S-V_D curves exhibits linear-like characteristics when the concentration of P3HT exceeds 0.8%. The total current in a polymeric TFT can be separated into two components, channel current (I_{ch}) and bulk current (I_{bk}).[11] Assuming the bulk current can be represented by Eq. 1 according to Ohm's law

$$I_{bulk} = \mu \frac{W}{L} l V_{DS} \qquad [1]$$

where μ is the carrier mobility and l is the thickness of the polymeric layer. Therefore, the observed linear-like off-state leakage is predominantly the bulk leakage current. The extracted thickness of P3HT film from Eq. 1 is around 100 nm, which also supports the above assumption.

To obtain an appropriate deposition concentration of P3HT, the dependence of the mobility and the ON/OFF current ratio *vs.* various weight percents of P3HT in chloroform were plotted in Fig. 5. Different device geometries were examined and the values of mobility or ON/OFF ratio were averaged using at least five points, all of them exhibiting a similar trends. There is a maximum value for ON/OFF ratio as concentration of P3HT equals 0.3%. Additionally, we inferred that the largest field-effect mobility would also occur at 0.3% because of the lowest value of surface roughness as shown in Fig. 2c. Although the peak value of mobility was located at 0.8% in Fig. 5, we speculated that the lower parasitic resistance for P3HT of 0.8% causes a slight over estimation of mobility. Besides, Aleshin *et al.* examined the electrical properties with respect to the P3HT concentration between 0.033 to 0.168% at extremely high spin speed.[19] At 0.06-0.07 wt %, the mobility is below 1×10^{-3} cm^2/Vs at room temperature but the ON/OFF ratio can exceed 10^5. Therefore, a trade-off should be made between mobility and off-state leakage current.

Downloaded on 2014-04-26 to IP 140.113.38.11 address. Redistribution subject to ECS terms of use (see ecsdl.org/site/terms_use) unless CC License in place (see abstract).

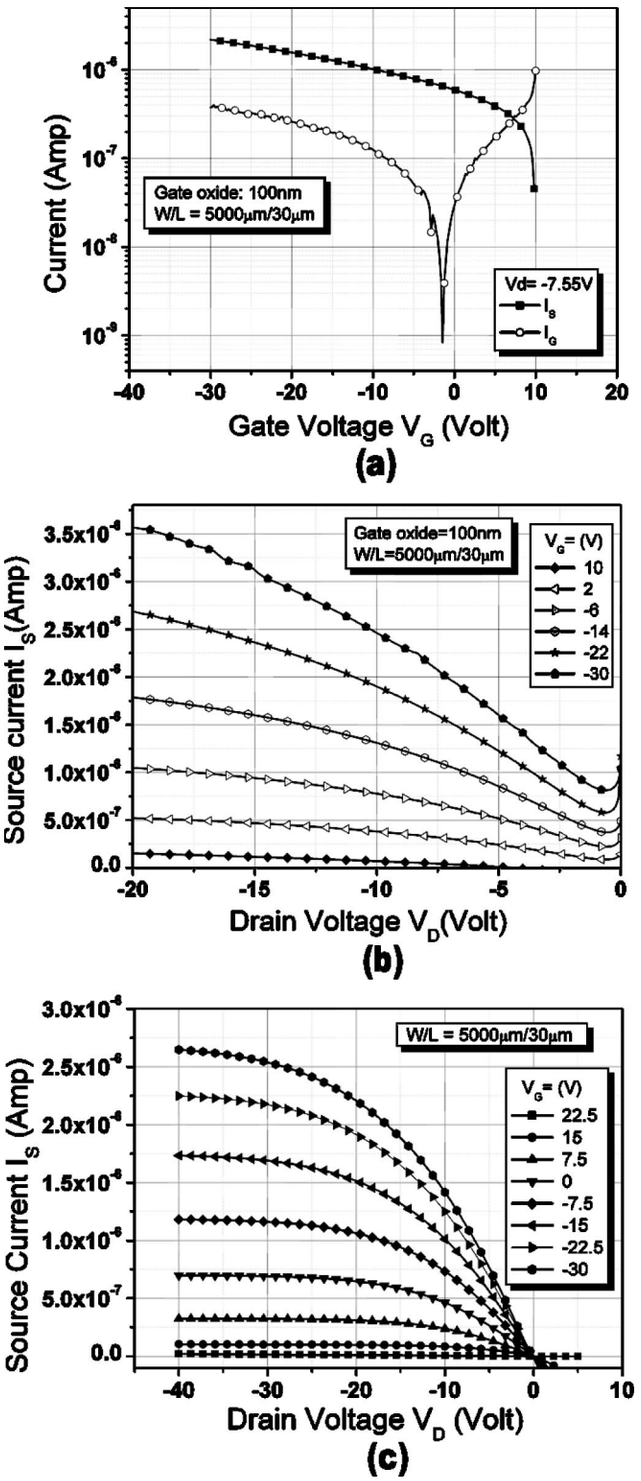

Figure 6. (a) I_S (I_G)-V_G and (b) I_S-V_D curves of the OTFTs without the field oxide layer, (c) I_S-V_D curves of the OTFTs with field oxide layer to eliminate the gate leakage current.

Anomalous leakage current.—The electrical characteristics of OTFTs without the thick field oxide layer as shown in Fig. 1c were plotted in Fig. 6a and b. Figure 6a compares the source current I_S and the gate leakage current I_G with the gate voltage V_G, while Fig. 6 b illustrates the I_S-V_D curves of the OTFTs. The gate leakage

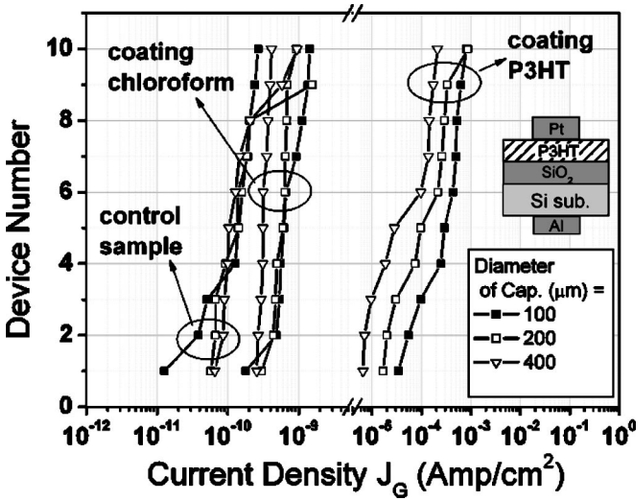

Figure 7. Comparison of gate leakage current density for MOS capacitors with different organic treatments.

current increases rapidly, becoming comparable to I_S as the magnitude of V_G increases. This anomalous leakage current not only deteriorates the electrical characteristics of transfer curves but also causes the overestimation of the device mobility. Moreover, the gate leakage is also responsible for the curve-splitting phenomenon in Fig. 6b at $V_D = 0$ V, making OTFT consume power continuously without an external drain bias.

To clarify the origin of the leakage current, metal oxide semiconductor (MOS) capacitors, as shown in the embedded part of Fig. 7 were fabricated, and then spun on chloroform or P3HT (0.3% wt in chloroform), respectively. Figure 7 plots the gate leakage current density (extracted at 2 MV/cm) of the MOS capacitors treated in various ways. Although the capacitor having been treated with chloroform exhibits almost the same electrical characteristics as the untreated capacitor, the leakage current density of MOS-C with P3HT is at least three orders of magnitude higher. The leakage current did not increase with the organic contamination such as chloroform. For MOS-C with P3HT treatment, it is also noticeable that the leakage current density distributes widely from 10^{-5} to 10^{-3} A/cm^2, and the leakage current density at $V_g = +40$ V is two orders of magnitude larger than that at $V_g = -40$ V. Accordingly, the additional leakage paths were assumed to be associated with the conductive P3HT film rather than the actual area of the top plate (Pt). Specifically, the conductive P3HT film connected the additional leakage paths of the insulator, increasing the effective area of the capacitor's top plate and, therefore, the leakage current; when a large negative gate bias was applied, the P3HT film became depleted and less conductive, contributing to a smaller effective area of the capacitor's top plate.

Two methods are available for alleviating the anomalous gate leakage in an OTFT. One is to pattern the active area, for which the P3HT can be dropped onto a specific place by microprinting technology, or can be etched away using UV light.[20,21] The second method, utilized in this work, is to form a thick field oxide layer on the wafer surface, except in the gate region. The leakage current density of the field oxide is lower than that of the thin-gate oxide; moreover, the P3HT film upon the field oxide does not accumulate and becomes less conductive as the (bottom) gate bias decreases. To reduce the process temperature, the field oxide layer can be fabricated by electron cyclotron resonance-plasma enhanced chemical vapor deposition (ECR-PECVD) or liquid-phase deposition system at room temperature without sacrificing the function of isolating structure.[22,23] As shown in Fig. 6c, the field oxide layer successfully eliminated the leakage current from the gate to the source/drain

Downloaded on 2014-04-26 to IP 140.113.38.11 address. Redistribution subject to ECS terms of use (see ecsdl.org/site/terms_use) unless CC License in place (see abstract).

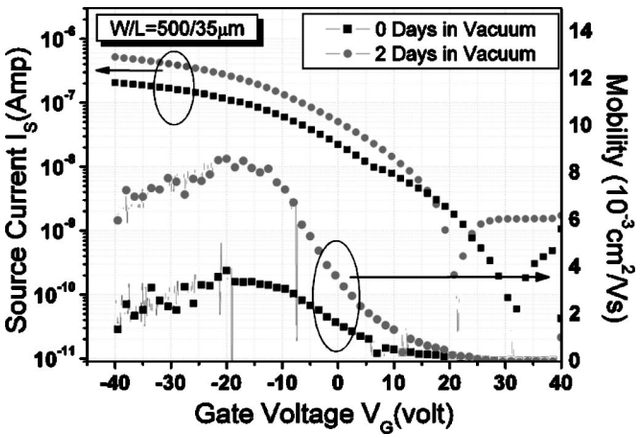

Figure 8. Electrical characteristics of an as fabricated OTFT and an OTFT after vacuum treatment for two days.

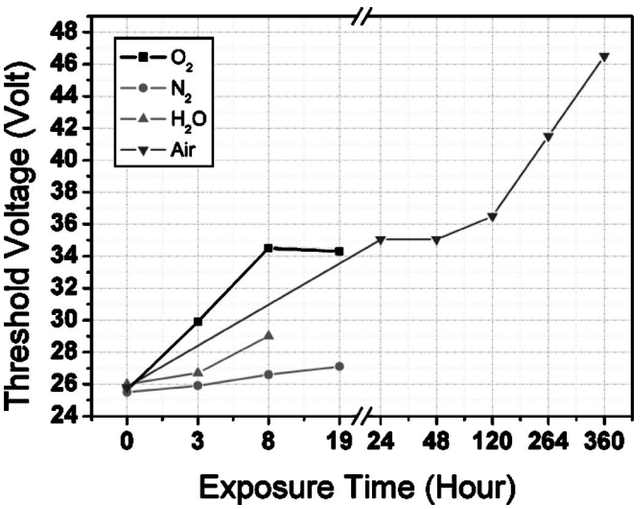

Figure 9. Threshold voltages *vs.* exposure time for OTFTs with O_2, N_2, H_2O, or air treatments.

electrodes, so no curve splitting phenomenon was observed at the origin of I_S-V_D curves.

Reliability tests of OTFTs.—Compared to an inorganic transistor, the organic devices are quite susceptible to oxygen or moisture in the atmosphere.[24] From either Fig. 3 or Fig. 4a, it can be found that the threshold voltage of OTFTs is larger than 20 V, implying that the devices are normally ON at zero gate bias. Since the spin-coating and measurement processes were performed in the air, the electrical characteristics of OTFTs would inevitably be influenced by O_2, H_2O, or N_2. Figure 8 compares the I_S-V_G curves for two samples, one was measured immediately after fabrication while the other was stored in a vacuum chamber ($<10^{-6}$ Torr) for two days after fabrication and then measured immediately in air. The threshold voltage was found to decrease from 28 to 18 V, and the mobility increased from 4×10^{-3} to 8×10^{-3} cm^2/V s after vacuum treatment, so the influences of the ambient condition, presumably the oxygen autodoping effect, can be partially reversed.[19]

To further clarify the origin of electrical property variation, the samples after being stored in a vacuum chamber were then treated with N_2/O_2 gas in a furnace or immersed in DI water; another samples were stored in the air in a moisture-proof cabinet with a relative humidity of 40% and their electrical properties were measured on the 1st, 2nd, 5th, 11th, 15th, and 30th days.

Figure 9 plots the threshold voltage of OTFTs *vs.* time. Clearly, the oxygen treatment caused the threshold voltage to increase significantly from 26 to 34 V within 8 h. As mentioned before, the oxygen atom is a kind of p-type dopant for P3HT. Therefore, the conductivity increases with oxygen incorporation, and a large gate voltage must be applied to fully deplete the channel region and turn the device OFF. Furthermore, because of oxygen reaching its solid-state solubility in P3HT, the threshold voltage gradually saturates at 36 V; another two weeks of exposure time is required for oxygen to diffuse to the interior of the P3HT film, resulting in V_{th} up to 46 V. We also found that the vacuum treatment is useless for samples exposed in the air over 24 h ($V_{th} > 30$ V) because the P3HT film had been seriously doped. Besides, when the V_{th} becomes too positive (>50 V), the operating voltage exceeds the breakdown field of the gate insulator, so the electrical properties of the OTFTs could not be measured on the 30th day.

In contrast to oxygen, both N_2 and H_2O treatments exhibit a negligible influence to the V_{th} shift of OTFTs. Because P3HT film is highly hydrophobic, we infer that the threshold voltage shift from 26 to 29 V after immersing in H_2O resulted from the dissolved O_2 in water and the device measurement processes.

The dependence of carrier mobility *vs.* different treatment conditions are illustrated in Fig. 10. For first 3 h, the mobility of OTFTs after O_2 treatment increased significantly since the conductivity and the associated parasitic source/drain series resistance decreased, contributing to an overestimation of mobility calculation. Meanwhile, the impurity scattering becomes more serious with increasing the oxygen doping concentration so that the carrier mobility declines continuously for a longer exposure time. For N_2 treatment, the mobility would also increase and then saturate owing to the out-diffusion of oxygen atoms, which is the case similar to the vacuum treatment. Moreover, although H_2O does not induce a significant shift of both threshold voltage and mobility, an abrupt yield loss was observed when the immersion time reaches 19 h. This may be attributed to the permeation of water through the pin holes of P3HT film and the creation of trap states at the P3HT/SiO_2 interface. Consequently, the investigation to figure out the detailed failure mechanism is still in progress.

Except O_2 or moisture, the V_{th} of OTFTs is also susceptible to the gate bias stress. To evaluate the electrical properties of OTFTs after stressing, we applied a gate bias of $+25$ V or -25 V while the source/drain were grounded for 0-2000 s. A control sample was also prepared to which no gate bias stress was applied, but the I_S-V_G

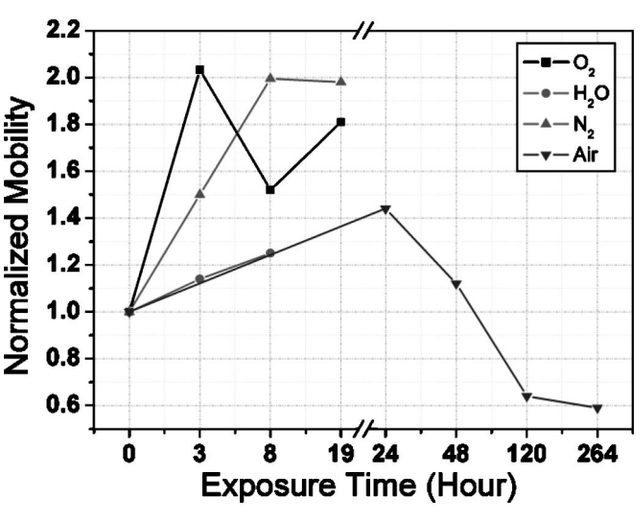

Figure 10. Normalized carrier mobility *vs.* exposure time for OTFTs with O_2, N_2, H_2O, or air treatments.

Downloaded on 2014-04-26 to IP 140.113.38.11 address. Redistribution subject to ECS terms of use (see ecsdl.org/site/terms_use) unless CC License in place (see abstract).

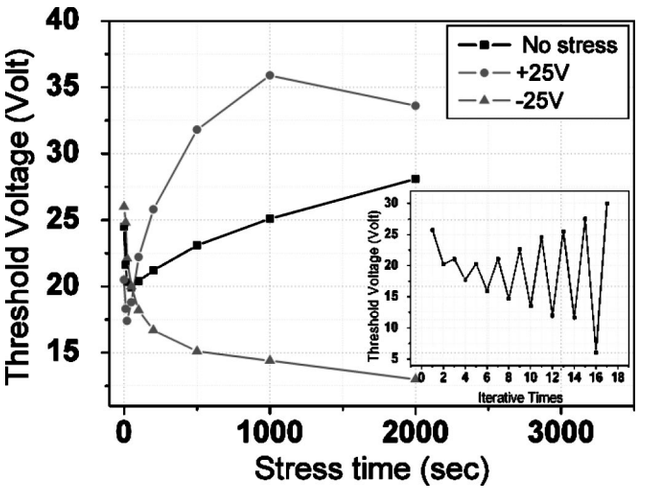

Figure 11. Threshold voltage shift of OTFTs with a constant +25 V/−25 V gate bias stresses and an alternative gate bias stress (insert).

curves (sweep V_G from +40 V to −40 V) were measured at the same time interval with those samples being stressed. As shown in Fig. 11, a positive V_{th} shift was observed after a +25 V gate bias stress and a negative V_{th} shift after a −25 V stress; for the control sample, a slight positive V_{th} shift can be found due to the oxygen autodoping effect during the measurement processes. Several mechanisms are responsible for the above observation, such as charge-trapping/relaxing near the semiconductor-insulator interface, mobile ions/trap-states in the high-*k* gate dielectric, or polarization effect. However, if the interface states were the dominant mechanism, the trap states would fill with holes under negative bias stress (because many holes now accumulate in the channel region) and then these filled trap states would not deteriorate the ON current during the following I_S-V_G measurement, *i.e.*, the V_{th} or current I_S should increase. But actually the V_{th} decreases under a negative bias stress. Similarly, a positive bias stress would deplete the trap states and then these empty states would trap the free holes during the following *I*-*V* measurement, causing a reduction of ON current, which also contradicts our observation. Besides, the gate insulator is a thermally grown SiO_2 and the *I*-*V* characteristics was measured at room temperature, so we can exclude the influence of mobile ions or oxide-trapped charges in the gate dielectric.

Using the concept of polarization can satisfactorily explain the results of gate bias stress. When the gate electrode was applied a constant negative bias, the dipoles from the polar part of P3HT molecules would rearrange and induce a polarization electric field as shown in Fig. 12a. The polarization electric field enhances the free holes to be depleted, and thus the device is easily turned off, and the threshold voltage would decrease. Similarly, as shown in Fig. 12b, the well-arranged dipoles and the induced polarization electric field under positive gate bias would enhance the accumulation of free holes. Therefore, the OTFT is easily turned ON while the threshold voltage would increase. Additionally, we stressed the samples with alternative gate bias, *e.g.*, V_G = 25 V for 10 s and V_G = −25 V for another 10 s, then V_G = 25 V for 20 s, −25 V for another 20 s, and so on. The results are shown in the embedded part of Fig. 11. The polarization phenomenon is fully reversible and not a degradation process. Accordingly, the hysteresis will not hinder use of the transistors in applications with a time scale of the order of seconds or tens of seconds, such as information recovery from a memory card or in applications with alternating polarity gate bias such as switches in active-matrix liquid-crystal displays.[15]

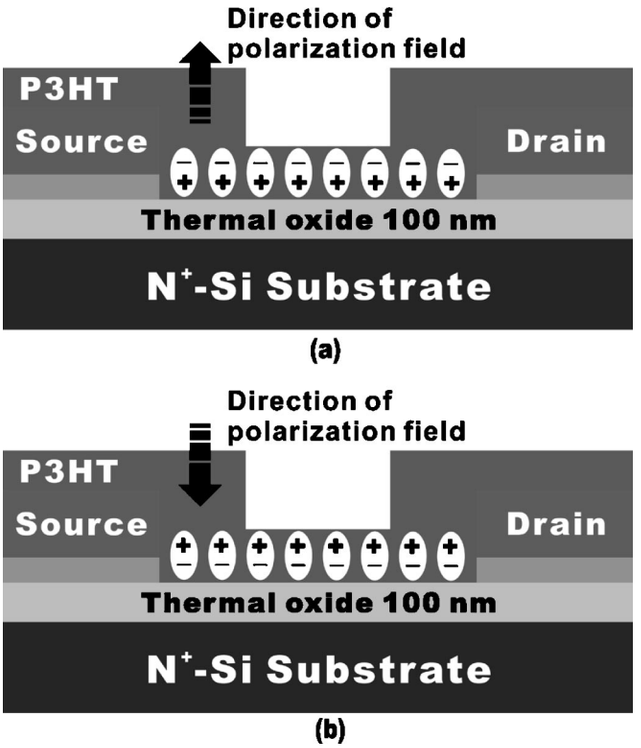

Figure 12. Direction of polarization electric field under a constant gate bias stress of (a) −25 V and (b) +25 V.

Conclusions

This study examined the physical properties of P3HT deposited with different solvents and weight percentages through AFM and SEM measurements. The P3HT film fabricated with a wt % of 0.3 in chloroform was found to exhibit the lowest surface roughness and high ON/Off current ratio and carrier mobility. The reason for the anomalous gate leakage current was clarified, and this current was eliminated by the thick field oxide layer on S/D regions. Moreover, through various post-treatment and long term storage tests, the impact of oxygen on the electrical characteristics of OTFTs is also explored. Finally, a polarization effect modal was proposed to explain the observed hysteresis phenomenon under gate bias stress.

Acknowledgments

The authors would like to thank their colleagues at Nano Facility Center in NCTU for their assistance in device fabrication. This work was supported by the National Science Council, Taiwan, under contract no. NSC92-2215-E-009-025

National Chiao-Tung University assisted in meeting the publication costs of this article.

References

1. J. H. Schön, C. Kloc, A. Dodabalapur, and B. Batlogg, *Science*, **289**, 599 (2000).
2. G. Horowitz, *Adv. Mater. (Weinheim, Ger.)*, **10**, 365 (1998).
3. A. Dodabalapur, Z. Bao, A. Makhija, J. G. Laquindanum, V. R. Raju, Y. Feng, H. E. Katz, and J. Rogers, *Appl. Phys. Lett.*, **73**, 142 (1998).
4. C. W. Tang, *Appl. Phys. Lett.*, **48**, 183 (1986).
5. G. Yu, Y. Cao, J. Wang, J. McElvian, and A. J. Heeger, *Synth. Met.*, **102**, 904 (1999).
6. T. Funamoto, Y. Matsueda, O. Yokoyama, A. Tsuda, H. Takeshita, and S. Miyashita, in *SID02 Digest*, 899 (2002).
7. A. Manuelli, A. Knobloch, A. Bernds, and W. Clemens, in *Proceedings of International IEEE Conference on Polytronics*, 23 (2002).
8. S. K. Park, Y. H. Kim, J. I. Han, D. G. Moon, W. K. Kim, and M. G. Kwak, *Synth. Met.*, **139**, 377 (2003).
9. H. Sirringhaus, N. Tessler, and R. H. Friend, *Science*, **280**, 1741 (1998).

Downloaded on 2014-04-26 to IP 140.113.38.11 address. Redistribution subject to ECS terms of use (see ecsdl.org/site/terms_use) unless CC License in place (see abstract).

10. B. A. Mattis, P. C. Chang, and V. Subramanian, *Mater. Res. Soc. Symp. Proc.*, **771**, L10.35.1 (2003).
11. M. S. A. Abdou, F. P. Orfino, Y. Son, and S. Holdcroft, *J. Am. Chem. Soc.*, **119**, 4518 (1997).
12. Z. T. Zhu, J. T. Mason, R. Dieckmann, and G. G. Malliaras, *Appl. Phys. Lett.*, **81**, 4643 (2002).
13. Y. Qiu, Y. Hu, G. Dong, L. Wang, J. Xie, and Y. Ma, *Appl. Phys. Lett.*, **83**, 1644 (2003).
14. W. A. Schoonveld, J. B. Oostinga, J. Vrijmoeth, and T. M. Klapwijk, *Synth. Met.*, **101**, 608 (1999).
15. A. R. Brown, C. P. Jarrett, D. M. de Leeuw, and M. Matters, *Synth. Met.*, **88**, 37 (1997).
16. G. Wang, D. Moses, and A. J. Heeger, *J. Appl. Phys.*, **95**, 316 (2004).
17. H. Sirringhaus, P. J. Brown, R. H. Friend, M. M. Nielsen, K. Bechgaard, B. M. W. Langeveld-Voss, A. J. H. Spiering, R. A. J. Janssen, E. W. Meijer, P. Herwig, and D. M. de Leeuw, *Nature (London)*, **401**, 14 (1999).
18. H. Kokubo, T. Yamamoto, H. Kondo, Y. Akiyama, and I. Fujimura, *Jpn. J. Appl. Phys., Part 1*, **42**, 6627 (2003).
19. A. N. Aleshin, H. Sandberg, and H. Stubb, *Synth. Met.*, **121**, 1449 (2001).
20. S. P. Speakman, G. G. Rozenberg, K. J. Clay, W. I. Milne, A. Ille, I. A. Gardner, E. Bresler, and J. H. G. Steinke, *Org. Electron.*, 2, 65 (2001).
21. T. K. S. Wong, S. Gao, X. Hu, H. Liu, Y. C. Chan, and Y. L. Lam, *Mater. Sci. Eng., B*, **55**, 71 (1998).
22. L. Teng and W. A. Anderson, *IEEE Electron Device Lett.*, **24**, 399 (2003).
23. C. F. Yeh, D. C. Chen, C. Y. Lu, C. Liu, S. T. Lee, C. H. Liu, and T. J. Chen, *Tech. Dig. - Int. Electron Devices Meet.*, **1998**, 269.
24. A. Lodha and R. Singh, *IEEE Trans. Semicond. Manuf.*, **14**, 281 (2001).

Downloaded on 2014-04-26 to IP 140.113.38.11 address. Redistribution subject to ECS terms of use (see ecsdl.org/site/terms_use) unless CC License in place (see abstract).